catalysts

MDPI

Supplementary Material

Figures of Merit for Photocatalysis: Comparison of NiO/La-$NaTaO_3$ and *Synechocystis* sp. PCC 6803 as a Semiconductor and a Bio-Photocatalyst for Water Splitting

Eike S. Welter [1], Sebastian Kött [1], Fabian Brandenburg [2], Jens Krömer [2], Michael Goepel [1], Andreas Schmid [2] and Roger Gläser [1,*]

1 Institute of Chemical Technology, Universität Leipzig, 04103 Leipzig, Germany; eike.welter@uni-leipzig.de (E.S.W.); sebastian.koett@uni-leipzig.de (S.K.); michael.goepel@uni-leipzig.de (M.G.), roger.glaeser@uni-leipzig.de (R.G.)
2 Department Solar Materials, Helmholtz Centre for Environmental Research—UFZ, 04318 Leipzig, Germany; fabian.brandenburg@ufz.de (F.B.); jens.kroemer@ufz.de (J.K.); andreas.schmid@ufz.de (A.S.)
* Correspondence: roger.glaeser@uni-leipzig.de

Abstract: While photocatalysis is considered a promising sustainable technology in the field of heterogeneous catalysis as well as biocatalysis, figures of merit (FOM) for comparing catalytic performance, especially between disciplines, are not well established. Here, photocatalytic water splitting was conducted using a semiconductor (NiO/La-$NaTaO_3$) and a bio-photocatalyst (*Synechocystis* sp. PCC 6803) in the same setup under similar reaction conditions, eliminating the often ill-defined influence of the setup on the FOMs obtained. Comparing the results enables the critical evaluation of existing FOMs and a quantitative comparison of both photocatalytic systems. A single FOM is insufficient to compare the photocatalysts, instead a combination of multiple FOMs (reaction rate, photocatalytic space time yield and a redefined apparent quantum yield) is superior for assessing a variety of photocatalytic systems.

Keywords: cyanobacteria; semiconductor; photocatalytic water splitting; figures of merit; *Synechcocystis* sp. PCC 6803; $NaTaO_3$

Citation: Welter, E.S.; Kött, S.; Brandenburg, F.; Krömer, J.; Goepel, M.; Schmid, A.; Gläser, R. Figures of Merit for Photocatalysis: Comparison of NiO/La-$NaTaO_3$ and *Synechocystis* sp. PCC 6803 as a Semiconductor and a Bio-Photocatalyst for Water Splitting. *Catalysts* **2021**, *11*, 1415. https://doi.org/10.3390/catal11111415

Academic Editor(s):Detlef W. Bahnemann; Ewa Kowalska; Ioannis Konstantinou; Magdalena Janus; Vincenzo Vaiano; Wonyong Choi; Zhi Jiang

Received: 30 October 2021
Accepted: 17 November 2021
Published: 22 November 2021

1. Figures-of-Merit

1.1. Influence of Photocatalyst Concentration

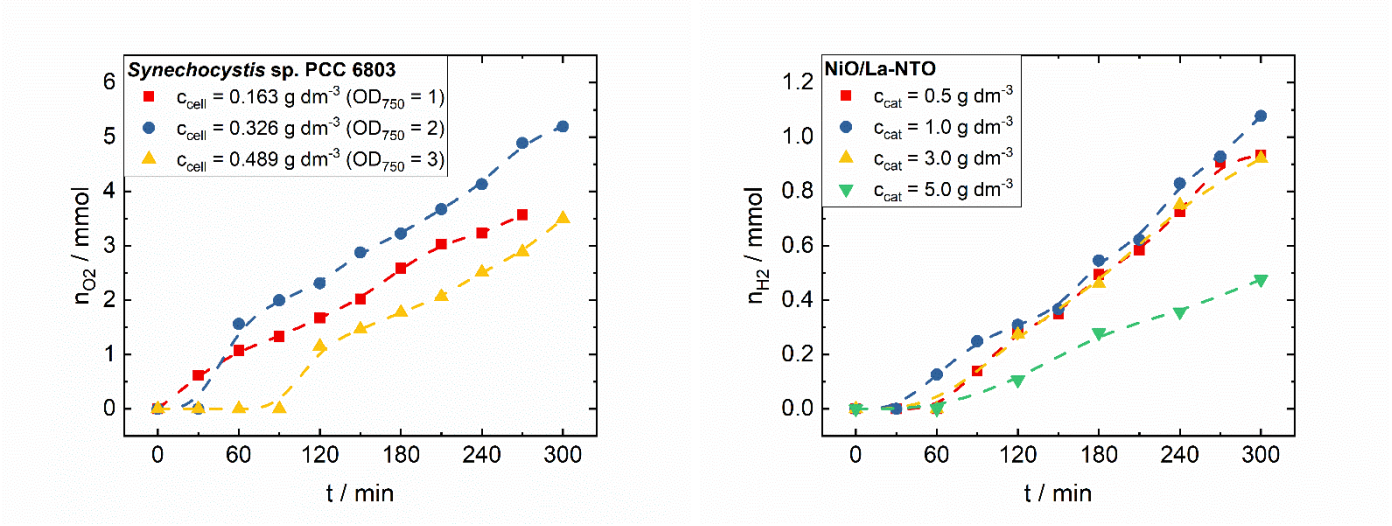

(**a**) (**b**)

Figure S1. O_2 evolution over *Synechocystis* (**a**) and H_2 evolution over NiO/La-NTO (**b**) as a function of time under full light spectrum (without a light filter) using 10 mW cm^{-2} and 200 mW cm^{-2} respectively. The catalyst concentration was varied from 0.163-0.489 g dm^{-3} (OD_{750} = 1-3) for the bio-photocatalyst and between 0.5-5 g dm^{-3} for the semiconductor photocatalyst.

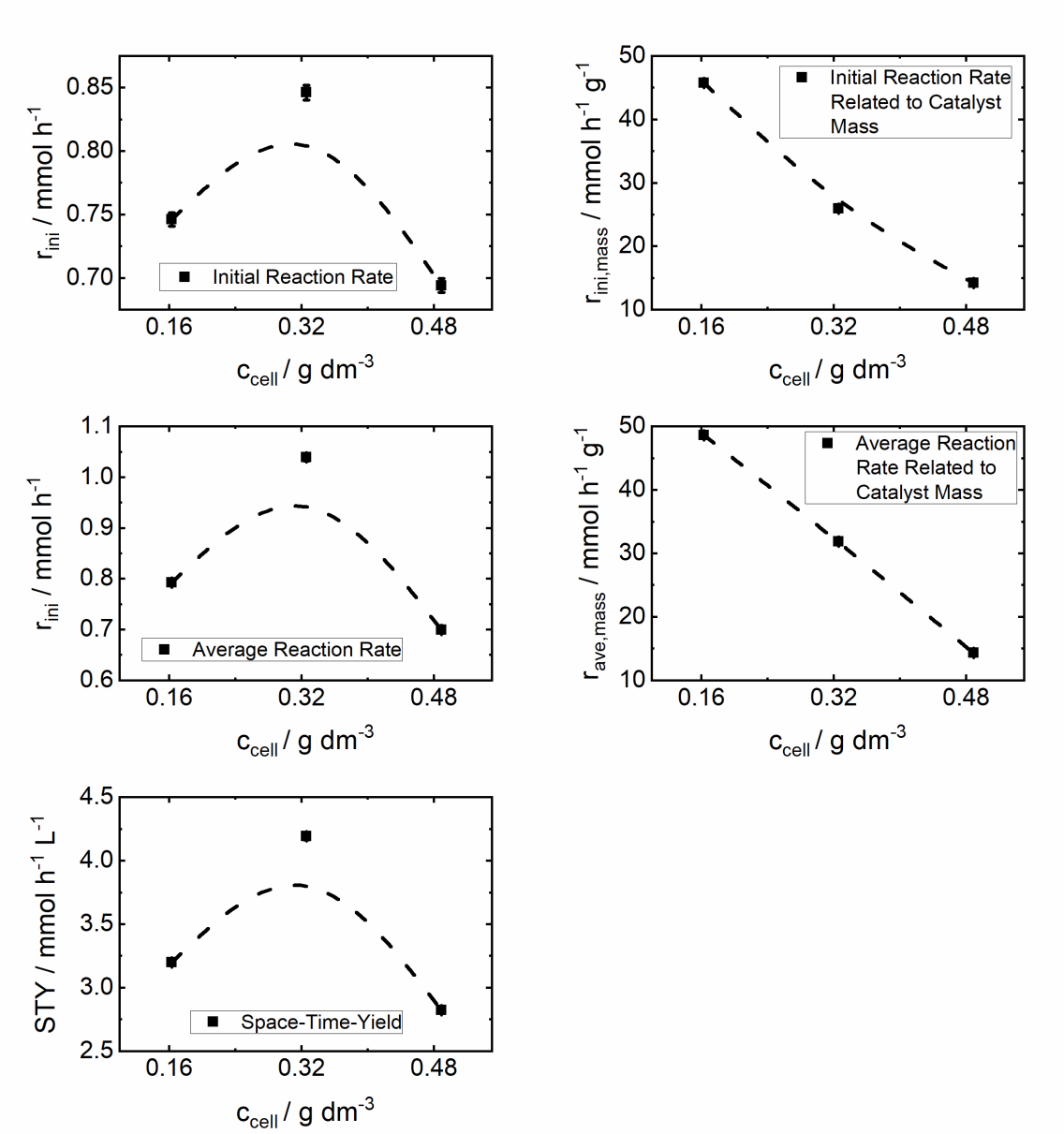

Figure S2. Dependence of the material-based Figures-of-Merit from the cell concentration of *Synechocystis* sp. PCC 6803 for the O_2 evolution from water splitting. The experiments were conducted with a light intensity of 10 mW cm^{-2}.

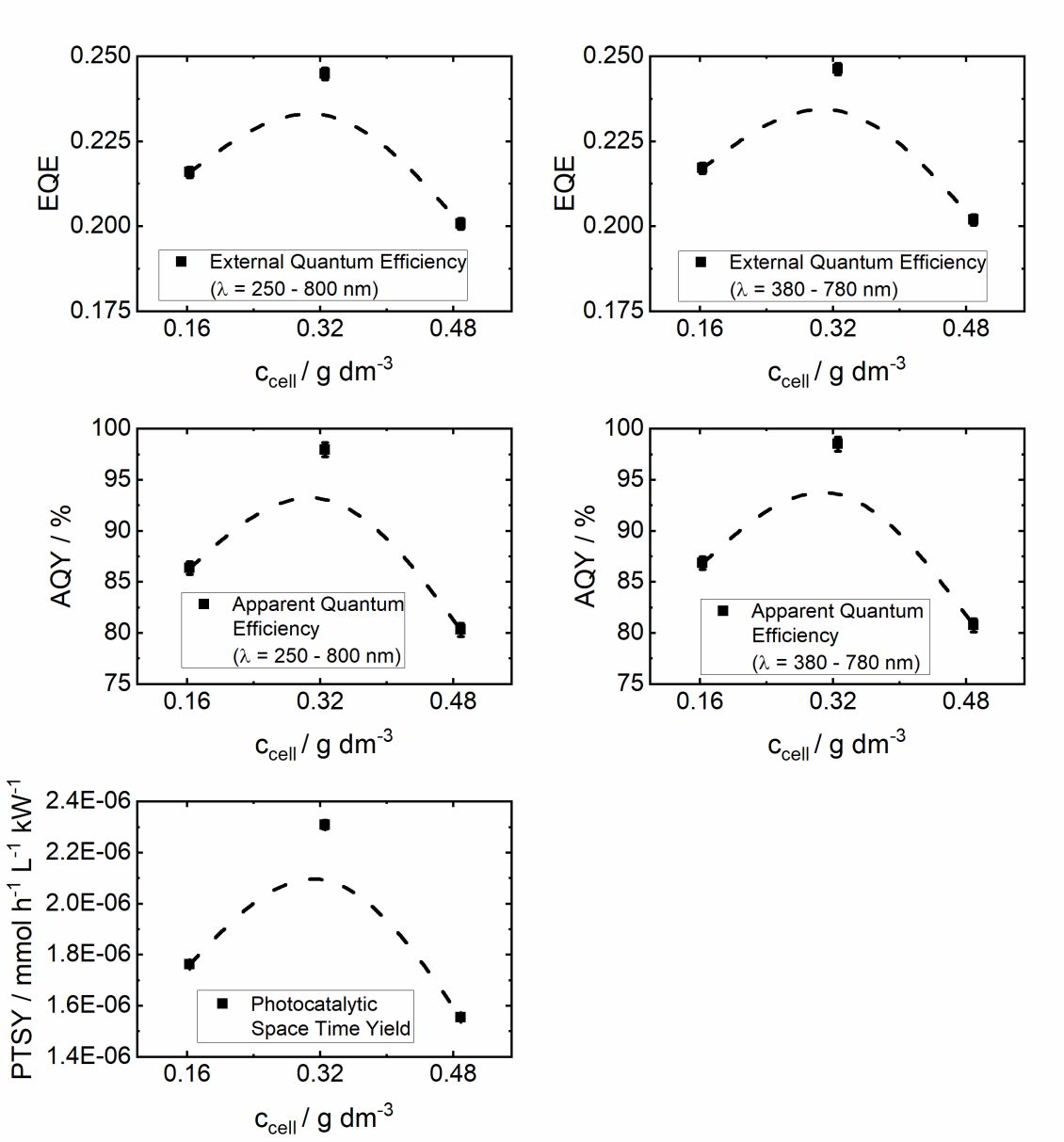

Figure S3. Dependence of the light-based Figures-of-Merit from the cell concentration of *Synechocystis* sp. PCC 6803 for the O_2 evolution from water splitting. The experiments were conducted with a light intensity of 10 mW cm^{-2}.

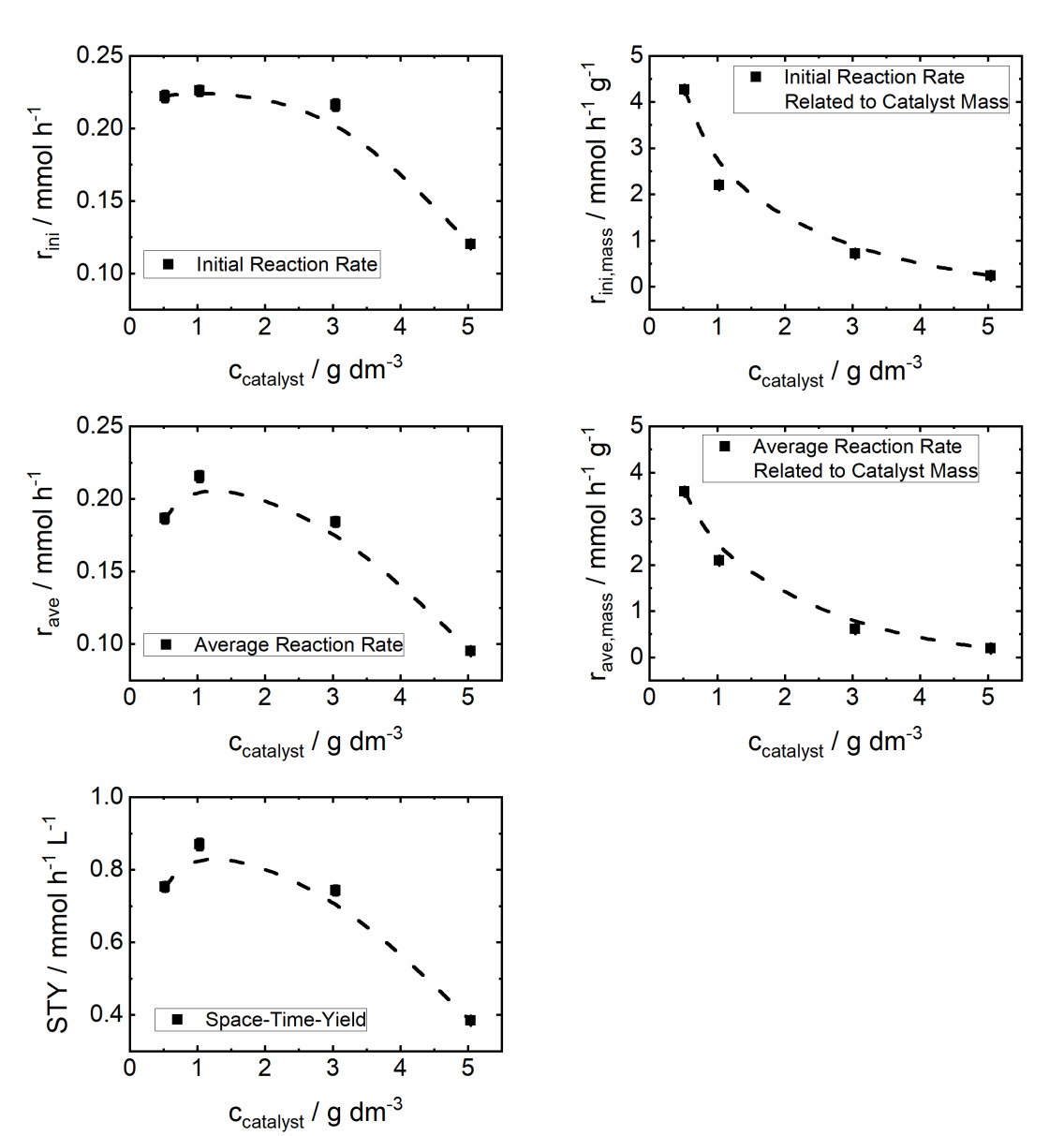

Figure S4. Dependence of the material-based Figures-of-Merit from the photocatalyst concentration of NiO/La-NTO for H_2 evolution from water splitting. The experiments were conducted with a light intensity of 200 mW cm^{-2}.

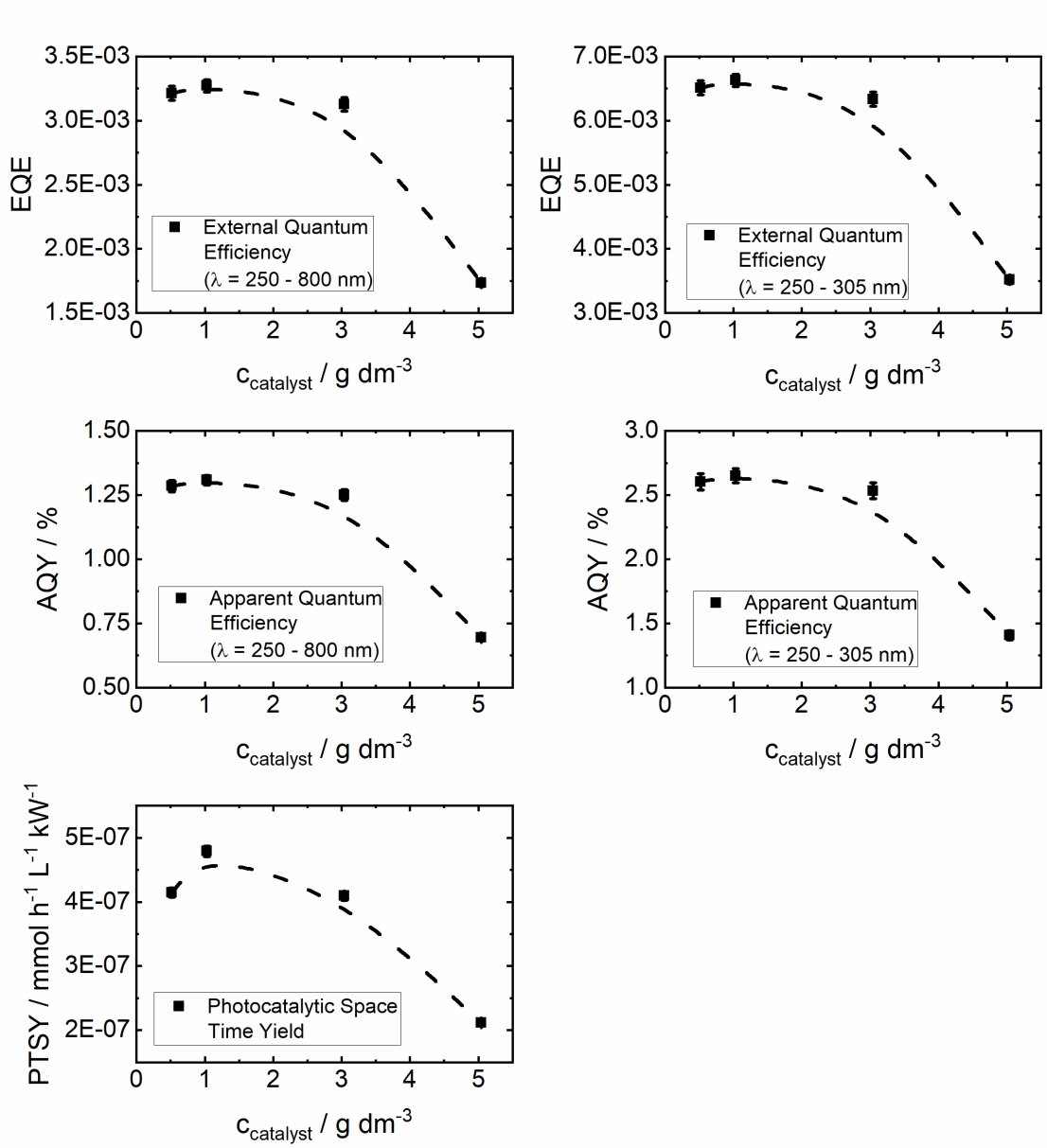

Figure S5. Dependence of the light-based Figures-of-Merit from the photocatalyst concentration of NiO/La-NTO for H_2 evolution from water splitting. The experiments were conducted with a light intensity of 200 mW cm^{-2}.

1.2. Influence of Light Spectrum and Intensity

1.2.1. Sunlight Spectrum

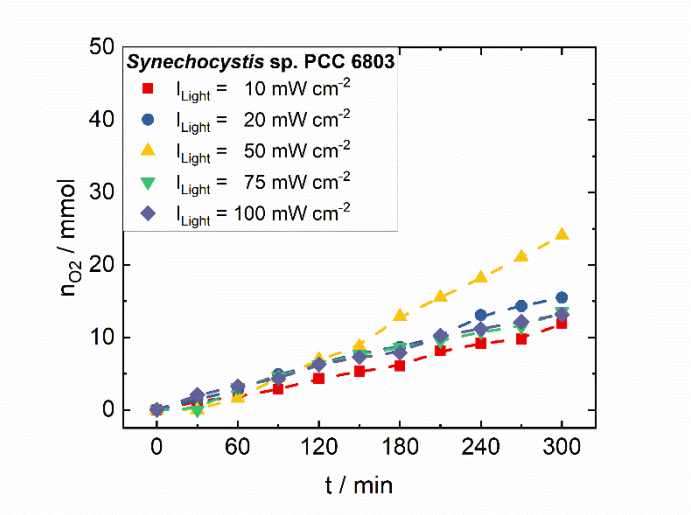

Figure S6. O_2 evolution as a function of time for *Synechocystis* using simulated sunlight (AM 1.5 filter) in the light intensity range of 10 to 100 mW cm^{-2} at cell concentration of 0.163 g dm^{-3}.

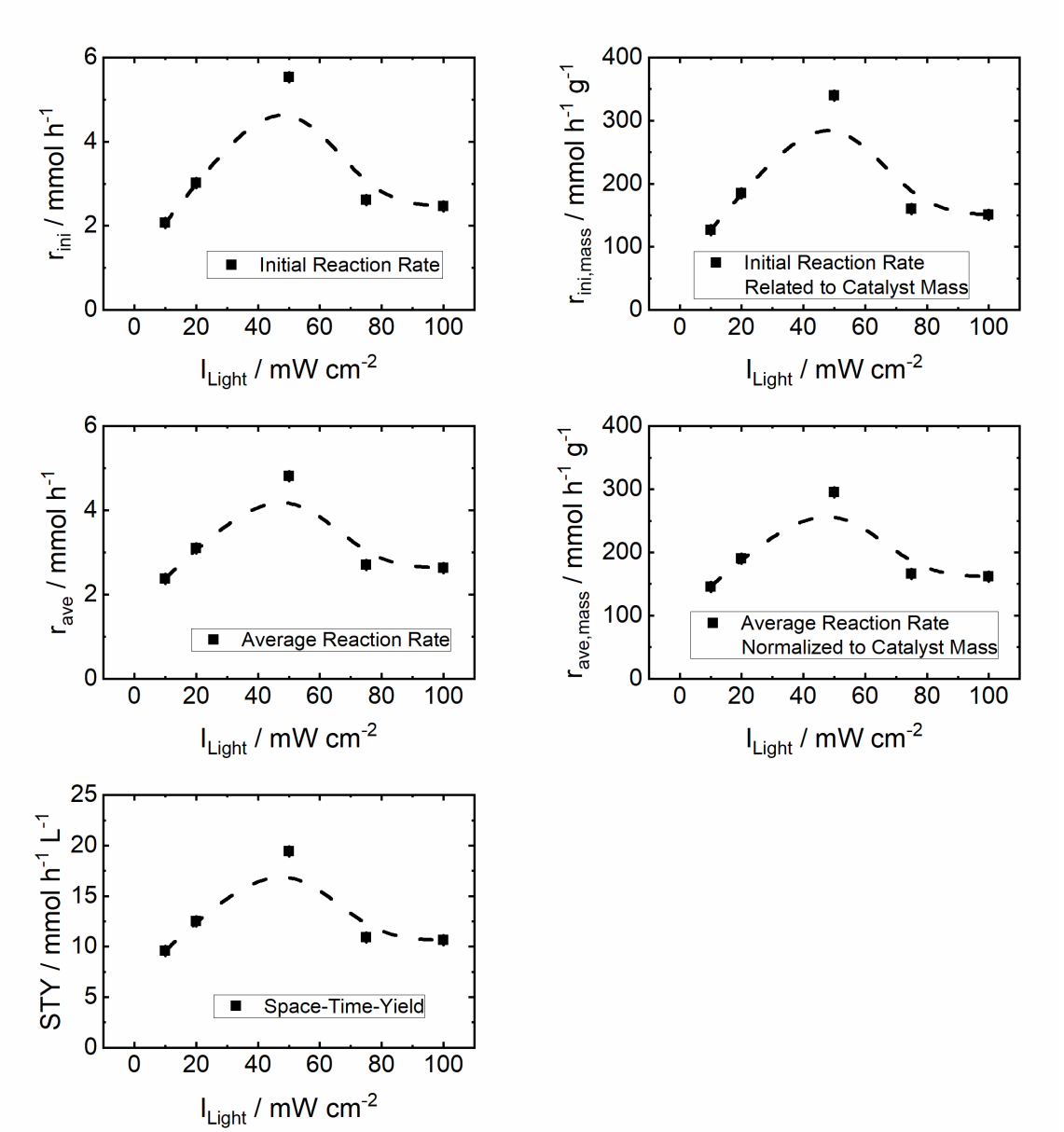

Figure S7. Dependence of the material-based Figures-of-Merit from the light intensity (AM 1.5G filter) for the O_2 evolution of *Synechocystis* sp. PCC 6803 from water splitting. The experiments were conducted with a cell concentration of 0.163 g $dm^{-3.}$

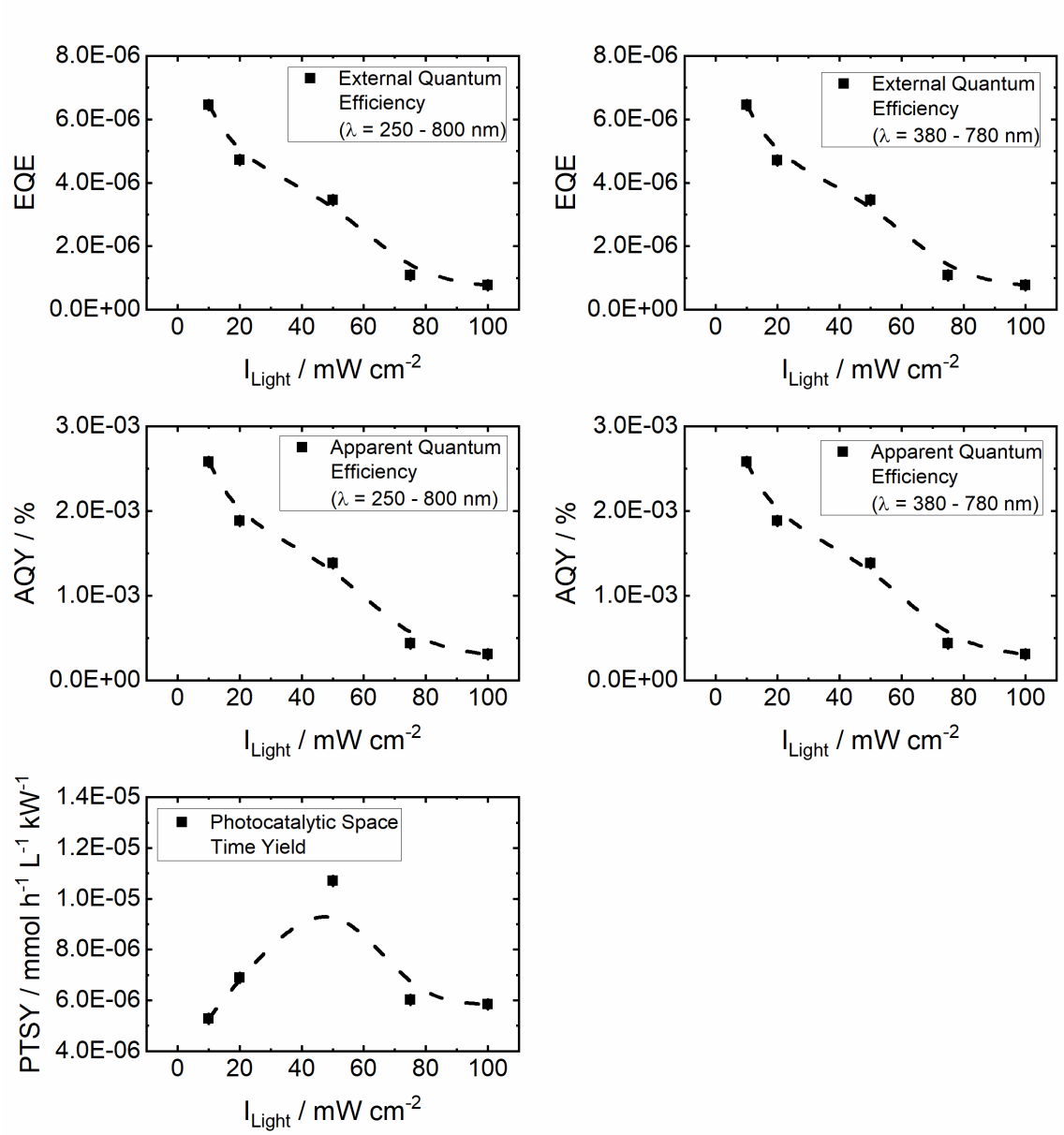

Figure S8. Dependence of the light-based Figures-of-Merit from the light intensity (AM 1.5G filter) for the O_2 evolution of *Synechocystis* sp. PCC 6803 from water splitting. The experiments were conducted with a cell concentration of 0.163 g dm^{-3}.

1.2.2. Full Lamp Light Spectrum

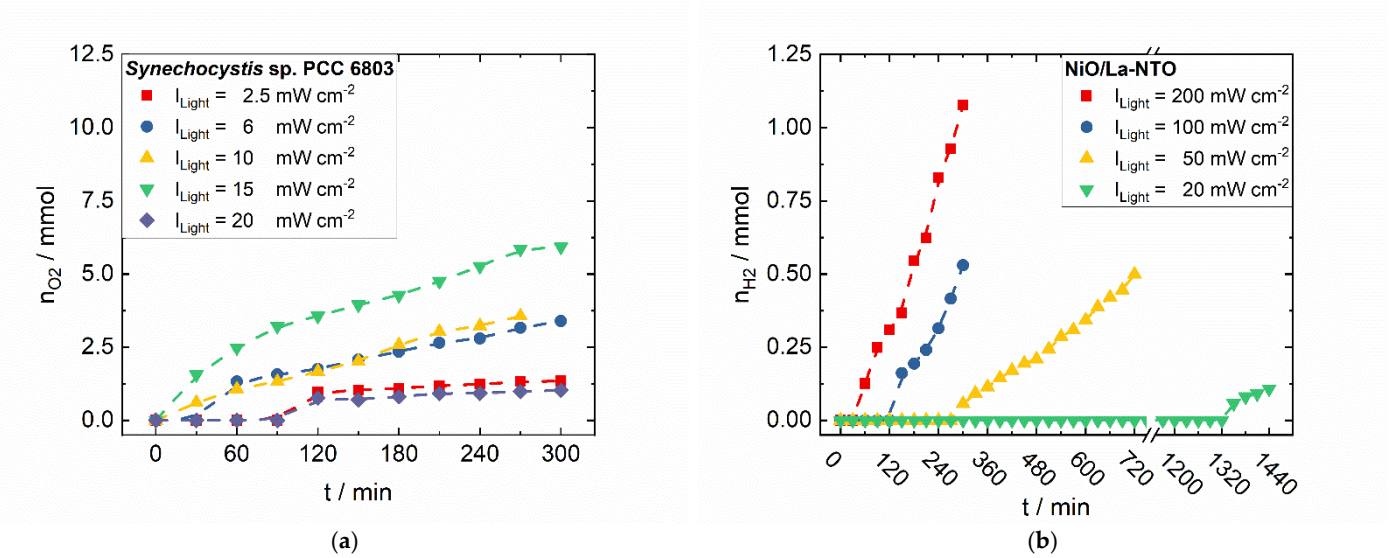

Figure S9. O_2 evolution of *Synechocystis* (**a**) and H_2 evolution of NiO/La-NTO (**b**) under full light spectrum (without a light filter) as a function of time using a cell concentration of 0.163 g dm^{-3} for the bacteria cells and a photocatalyst concentration of 1 g dm^{-3} for the semiconductor. The light intensity was varied in the range of 2.5 to 20 mW cm^{-2} and 20 to 200 mW cm^{-2} respectively.

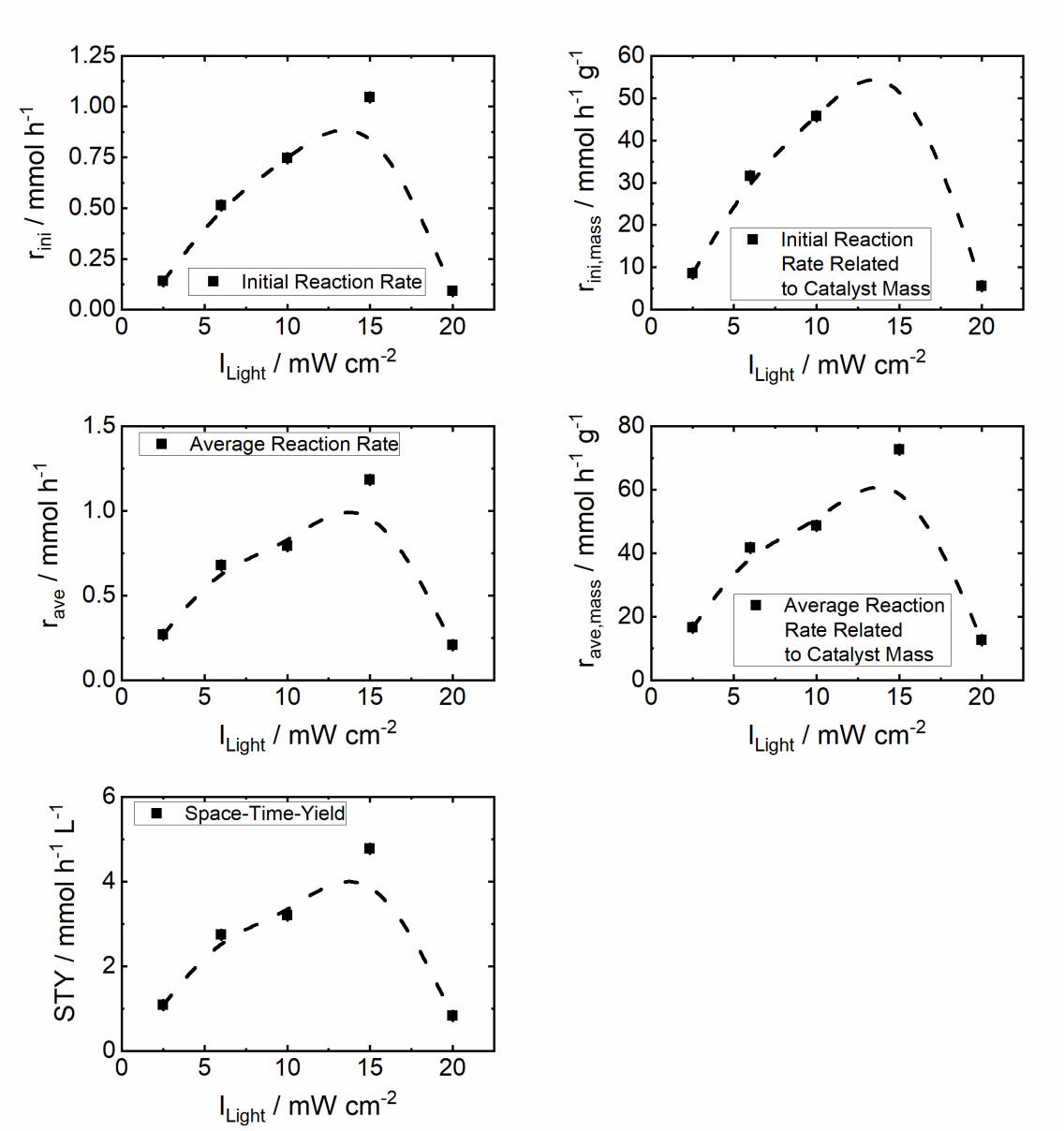

Figure S10. Dependence of the material-based Figures-of-Merit from the light intensity (no filter) for the O_2 evolution of *Synechocystis* sp. PCC 6803 from water splitting. The experiments were conducted with a cell concentration of 0.163 g dm^{-3}.

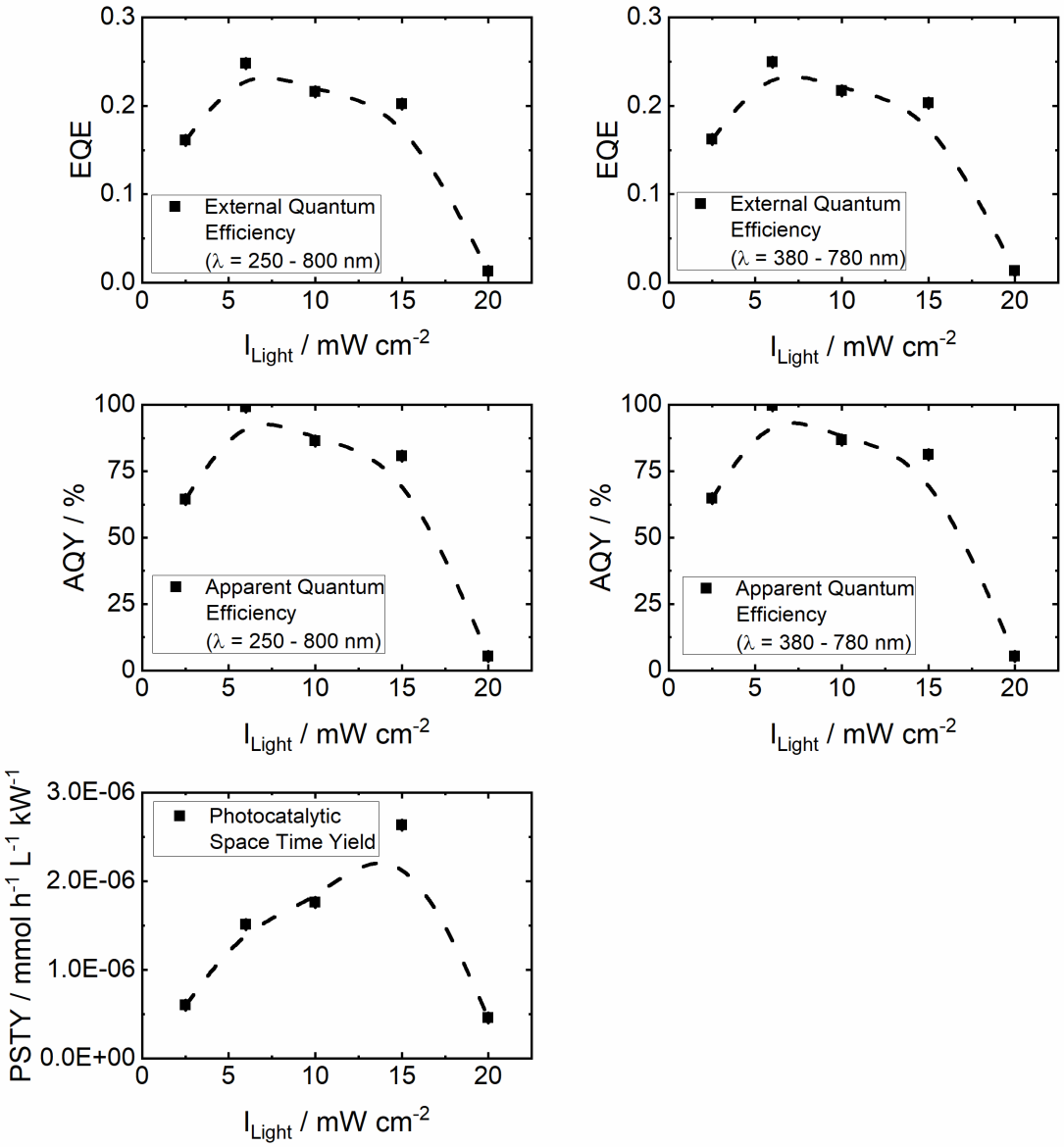

Figure S11. Dependence of the light-based Figures-of-Merit from the light intensity (no filter) for the O_2 evolution of *Scheme 6803.* from water splitting. The experiments were conducted with a cell concentration of 0.163 g dm^{-3}.

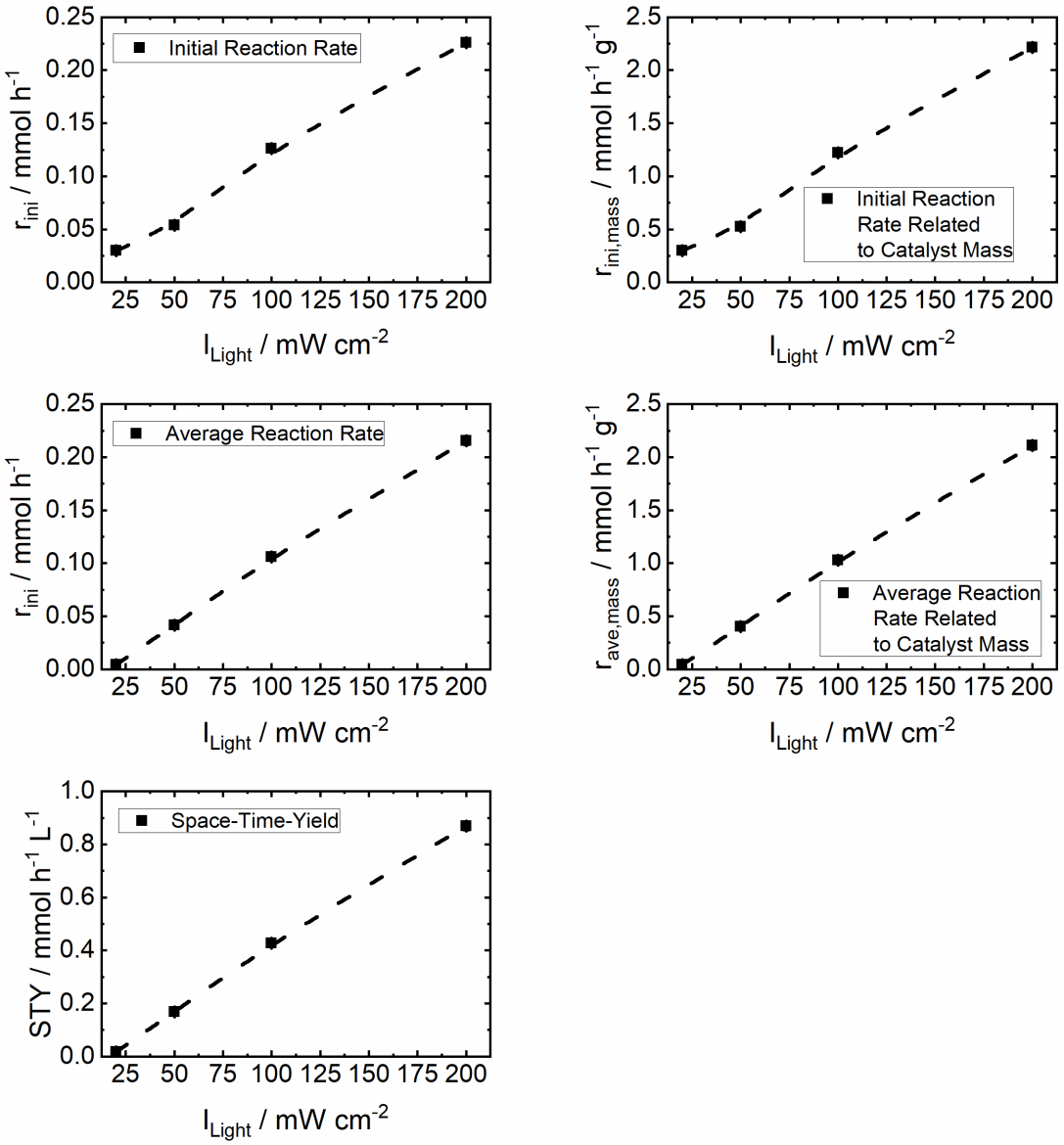

Figure S12. Dependence of the material-based Figures-of-Merit from the light intensity (no filter) for the H_2 evolution of NiO/La-NTO from water splitting. The experiments were conducted with a photocatalyst concentration of 1 g dm^{-3}.

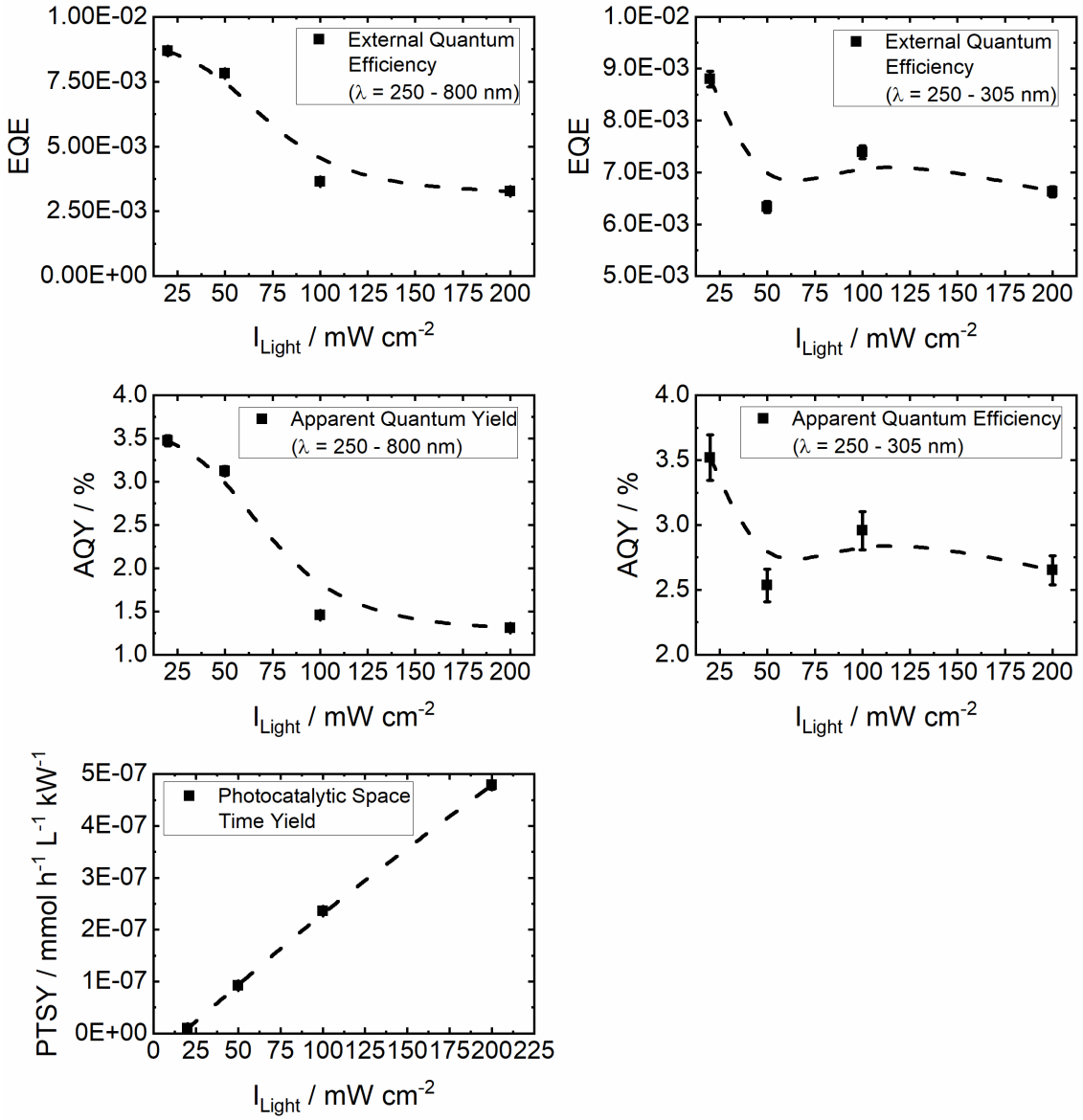

Figure S12. Dependence of the light-based Figures-of-Merit from the light intensity (no filter) for the H_2 evolution of NiO/La-NTO from water splitting. The experiments were conducted with a photocatalyst concentration of 1 g dm^{-3}.

1.3. Comparison of NiO/La-NTO and Synechocystis

1.3.1. Maximum Product Evolution Rate

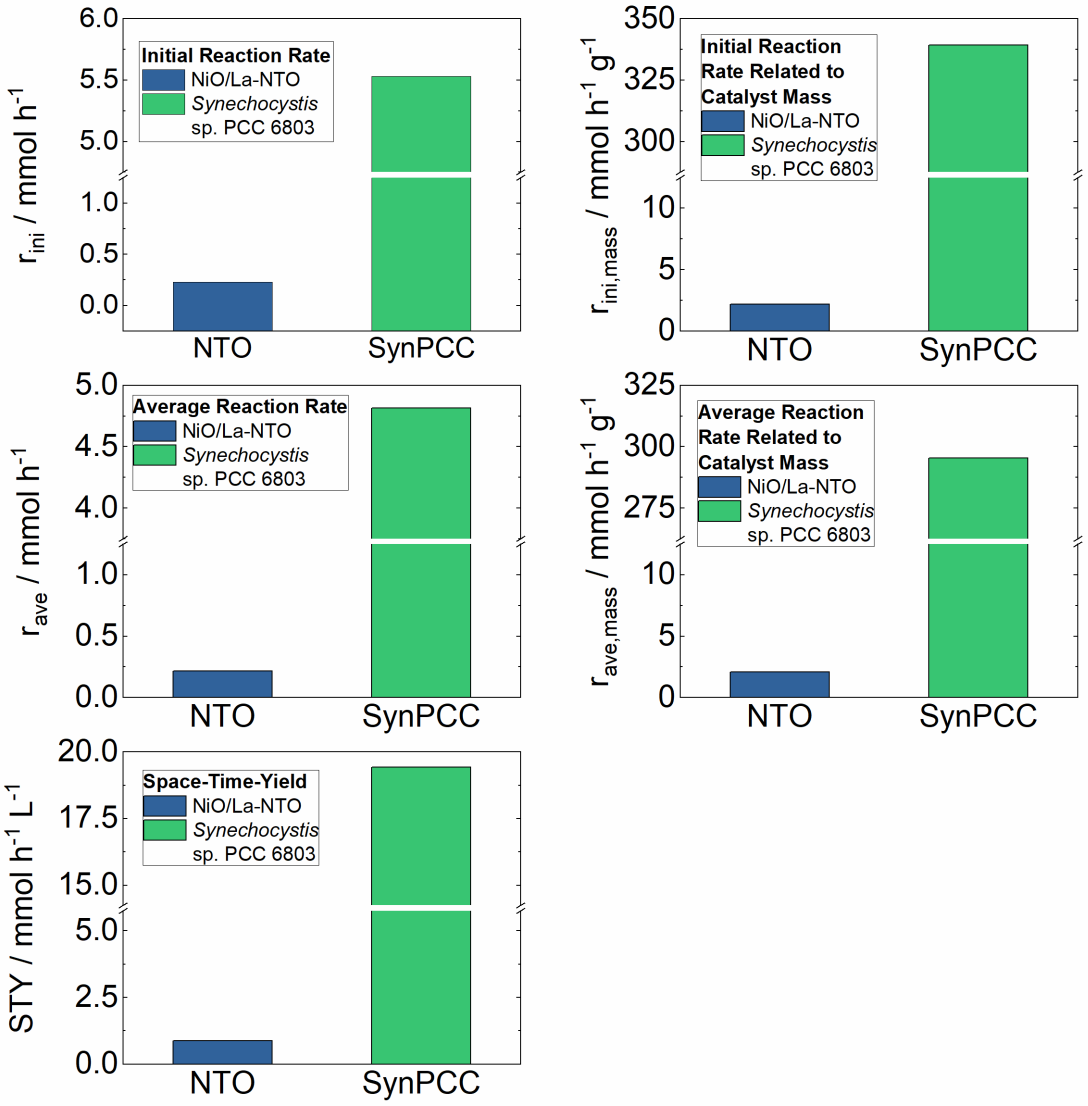

Figure S13. Material-based Figures-of-Merit for *Synechocystis* sp. PCC 6803 and NiO/La-NTO at maximum product evolution rate of this study (Synechocystis sp. PCC 6803: c_{cell} = 0.163 g dm^{-3}, I_{light} = 50 mW cm^{-2}, AM 1.5G filter; NiO/La-NTO: c_{cat} = 1 g dm^{-3}, I_{light} = 200 mW cm^{-2}, no filter).

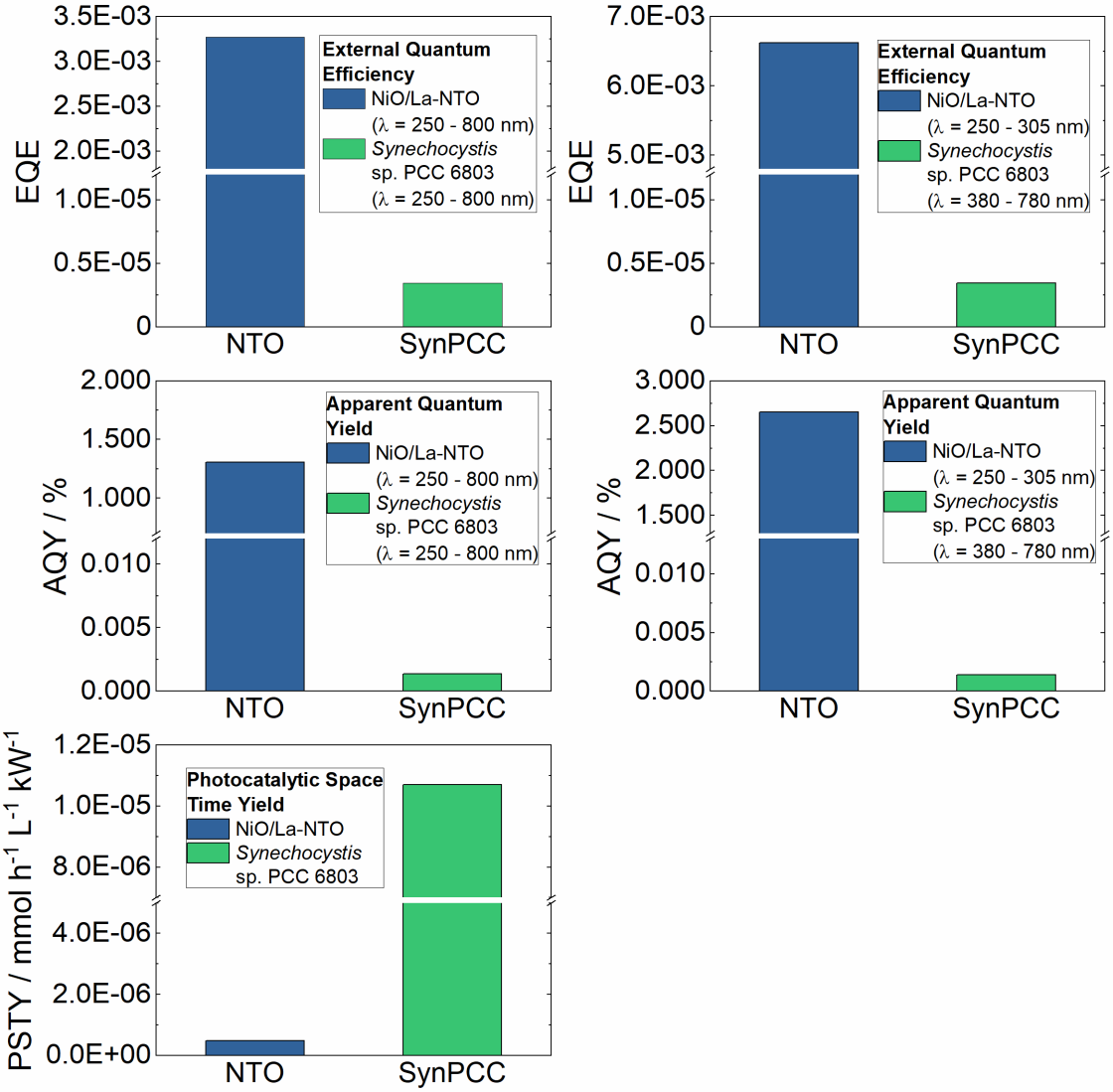

Figure S14. Light-based Figures-of-Merit for *Synechocystis* sp. PCC 6803 and NiO/La-NTO at maximum product evoluTable 6803. c_{cell} = 0.163 g dm^{-3}, I_{light} = 50 mW cm^{-2}, AM 1.5G filter; NiO/La-NTO: c_{cat} = 1 g dm^{-3}, I_{light} = 200 mW cm^{-2}, no filter).

1.3.2. Similar Illumination Conditions

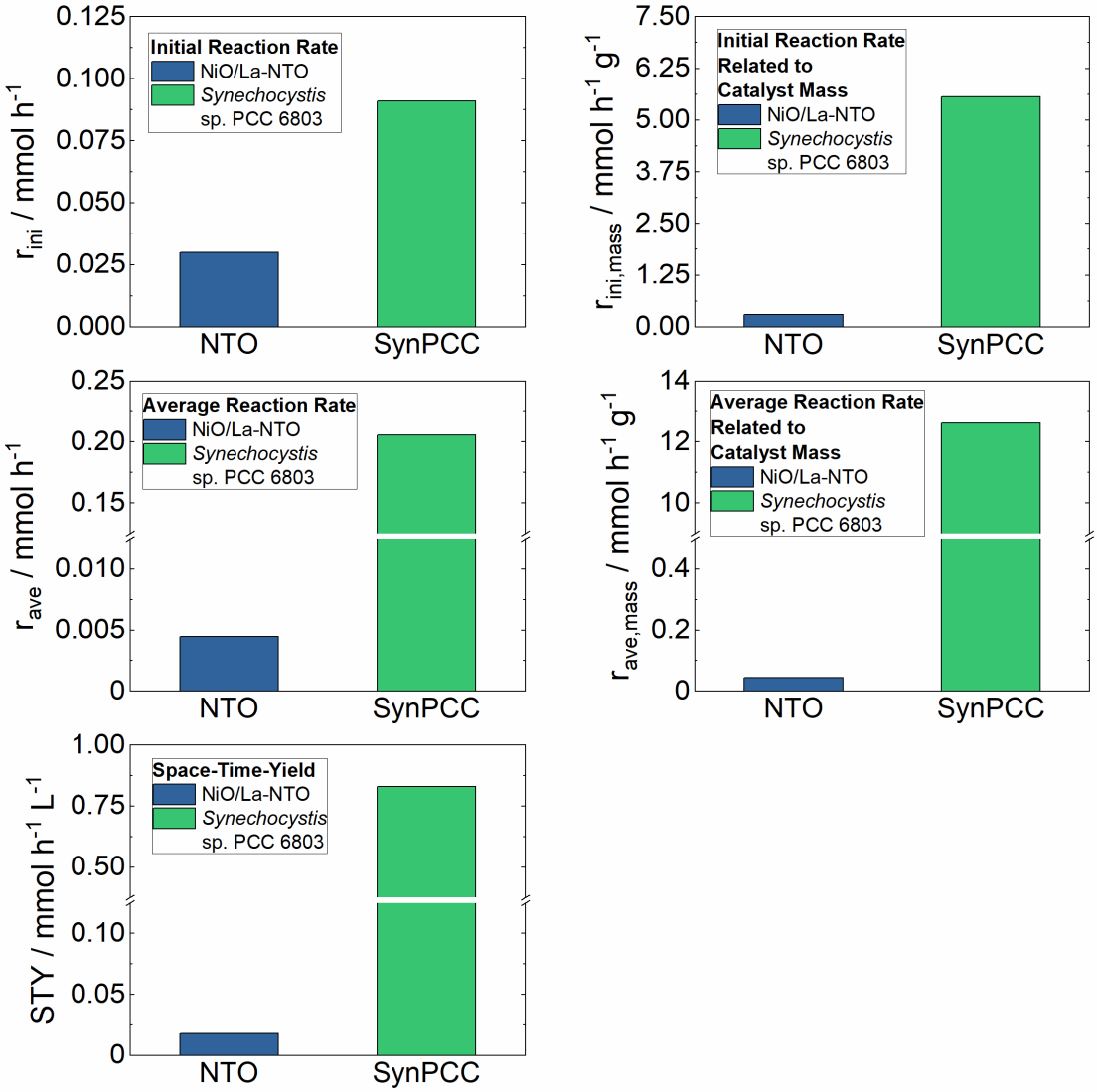

Figure S16. Material-based Figures-of-Merit for *Synechocystis* sp. PCC 6803 and NiO/La-NTO at similar illumination conditions (Synechocystis sp. PCC 6803: c_{cell} = 0.163 g dm^{-3}, I_{light} = 20 mW cm^{-2}, no filter; NiO/La-NTO: c_{cat} = 1 g dm^{-3}, I_{light} = 20 mW cm^{-2}, no filter).

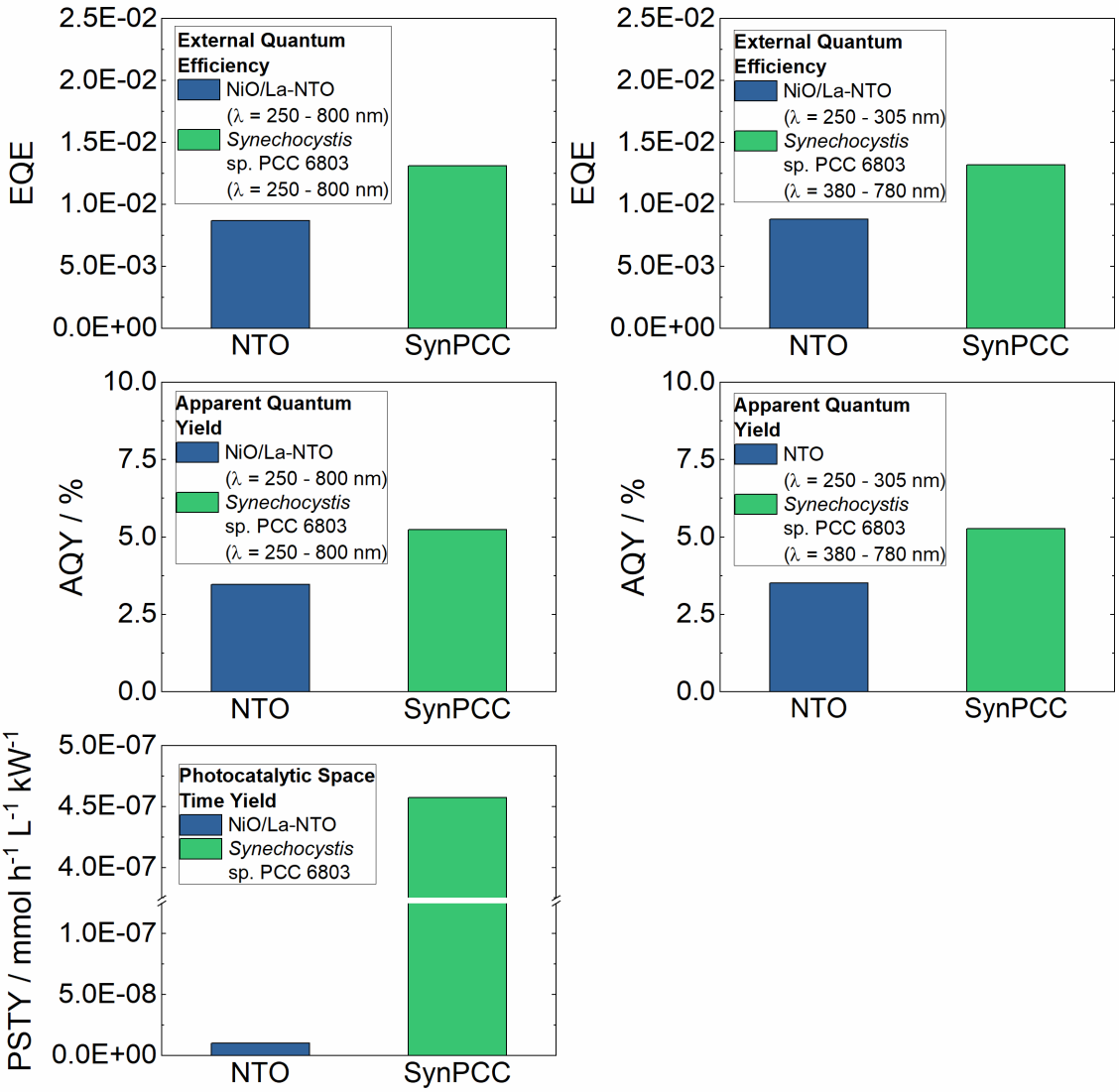

Figure S17. Light-based Figures-of-Merit for *Synechocystis* sp. PCC 6803 and NiO/La-NTO at similar illumination conditions (Synechocystis sp. PCC 6803: c_{cell} = 0.163 g dm^{-3}, I_{light} = 20 mW cm^{-2}, no filter; NiO/La-NTO: c_{cat} = 1 g dm^{-3}, I_{light} = 20 mW cm^{-2}, no filter).

1.3.3. Photocatalyst Stability

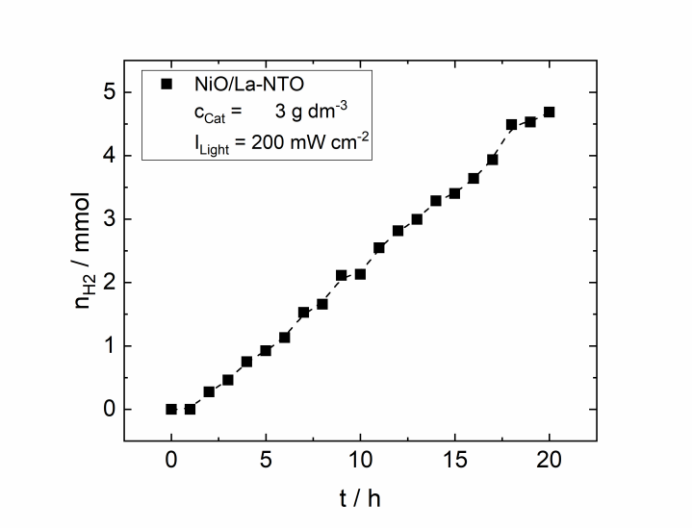

Figure S18. H_2 evolution over NiO/La-NTO using a c_{cat} of 3 g dm^{-3} and I_{Light} of 200 mW cm^{-2}.

2. Semiconductor Characterization

2.1. Elemental Analysis

The Ni-content after the impregnation procedure was determined by optical emission spectroscopy with inductively coupled plasma (ICP-OES) using a Perkin Elmer Optima 8000 with Ar plasma and a Scott/Cross-Flow atomizer. Solid samples were placed in a PTFE vessel in a mixture of 2 cm^3 aqueous HF (48%, Merck), 3 cm^3 aqueous HNO_3 (69%, Roth), 3 cm^3 aqueous HCl (35%, Roth) prior to analysis, and digested with the help of microwave treatment (microwave oven, Anton Parr Multiwave 3000, 8 XF100 rotor) at 533 K for 30 min with a heating rate of 15 K min^{-1}. After digestion the resulting solution was diluted 1:50 (V_{Sample}:V_{H2O}) with ultrapure H_2O (Elga, 0.055 µS).

2.2. Powder X-Ray Diffraction

Powder XRD patterns were recorded at room temperature using a Siemens, D5000 diffractometer. The diffracted intensity of Cu-K_α radiation (λ = 0.154 nm) was measured in the range of 2θ between 4° and 90°, with a step size of 0.005° and a counting time of 0.2 s for crystal structure determination.

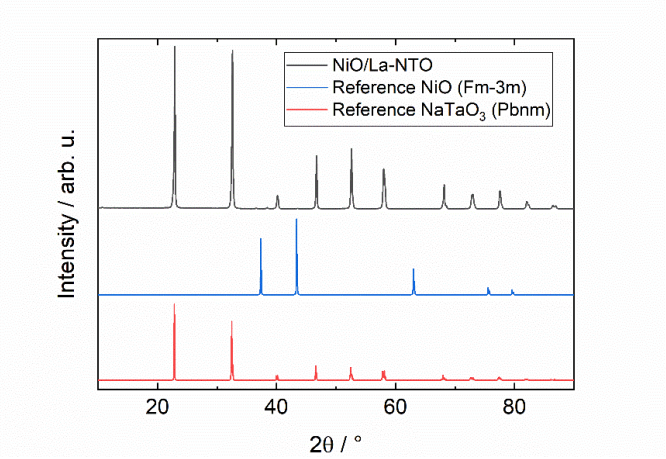

Figure S19. X-Ray powder diffraction pattern of NiO/La-NTO (black), reference patterns of NiO (blue) [1] and $NaTaO_3$ (red) [2] in the space group Fm-3m and Pbnm respectively.

2.3. UV/Vis Diffuse Reflectance Spectroscopy

UV/Vis diffuse reflectance spectra were recorded using a Lambda 650S UV/Vis spectrophotometer (Perkin Elmer) equipped with an integration sphere (150 mm). The spectra were recorded from 250 nm to 800 nm with a step width of 1 nm and a slit width of 2 nm. As a reference we used Spectralon® standard (Labsphere).

The band gap was determined via the theory of Kubelka-Munk. Therefore, the experimentally measured reflection R was converted to the remission F(R) using eq. (1). The band gap was then determined graphically from a plot of F(R) against photon energy (h(ν)), with the intersection of the linear fit of the slope with the x-axis corresponding to the energy of the band gap.

$$F(R) = \frac{(1-R)}{2R} = \frac{k}{s} \quad (1)$$

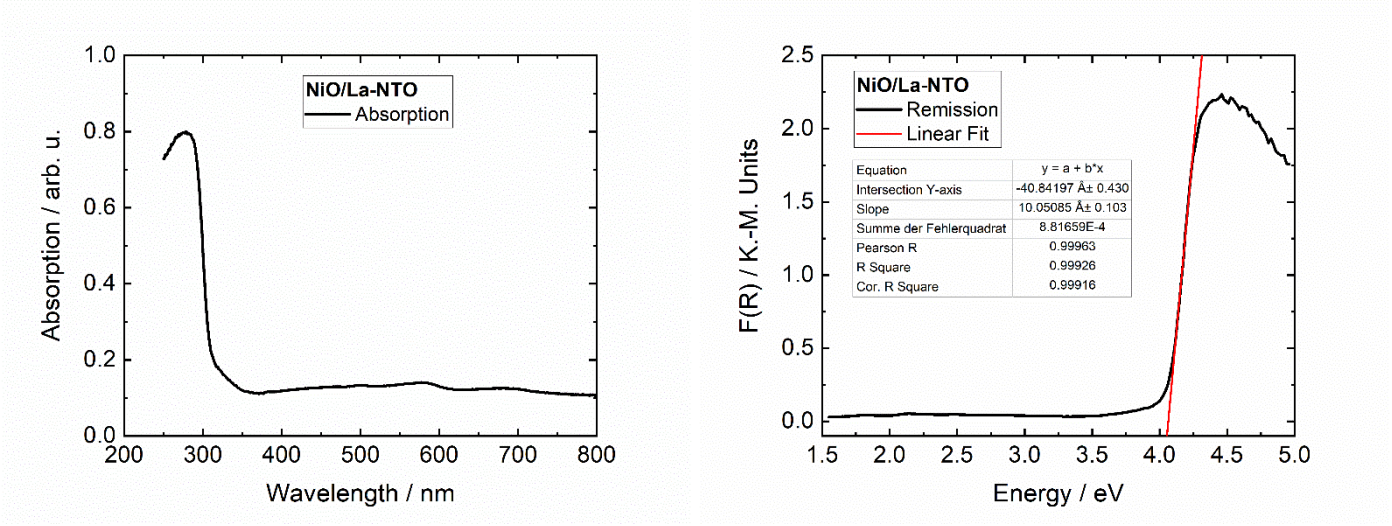

(**a**) (**b**)

Figure S20. UV/Vis diffuse reflection spectrum of NiO/La-NTO (**a**) and the resulting Kubelka-Munk transformation (**b**) used for the determination of the band gap by linear regression of the slope.

2.4. Transmission Electron Microscopy

TEM imaging was performed using a Jeol JEM2100Plus equipped with a LaB_6 electron gun operated at 200 keV to obtain 0.23 nm point resolution. The microscope is equipped with an ultrafast 4K CMOS camera TemCam-F416 (TVIPS) for high resolution imaging. Image processing was done by the corresponding EM-Menu software. Chemical analysis was performed by an energy dispersive X-ray detector Octane SDD (EDAX) and data evaluation and quantification by TEAM Enhanced software package (EDAX). Sample preparation for TEM investigation was done by grinding, suspension in ethanol and transferring to TEM holey carbon grid.

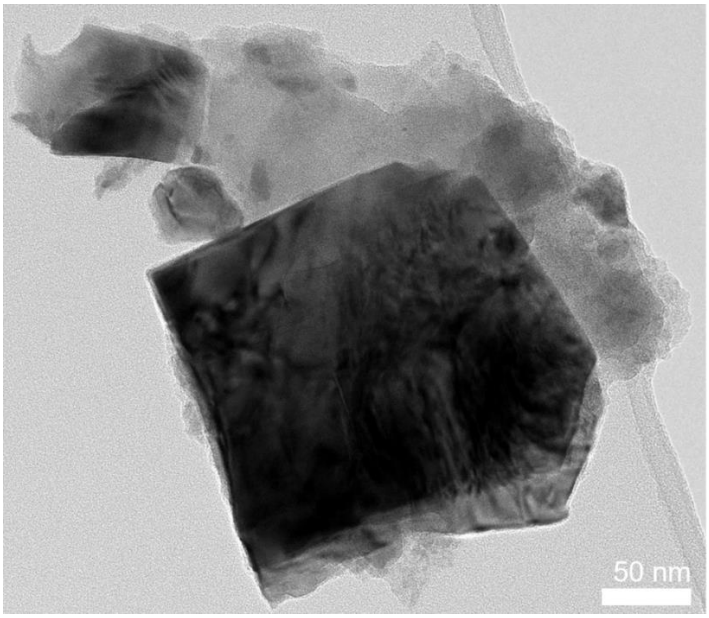

Figure S21. TEM image of NiO/La-NTO.

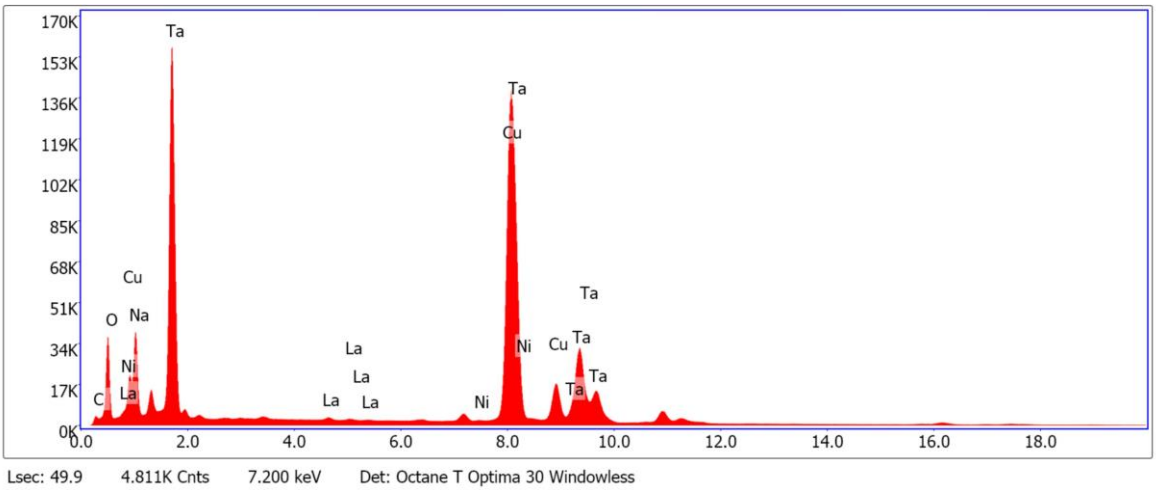

Figure S22. TEM-EDX spectrum of NiO/La-NTO used for the determination of La-content.

3. Bio-Photocatalyst Characterization

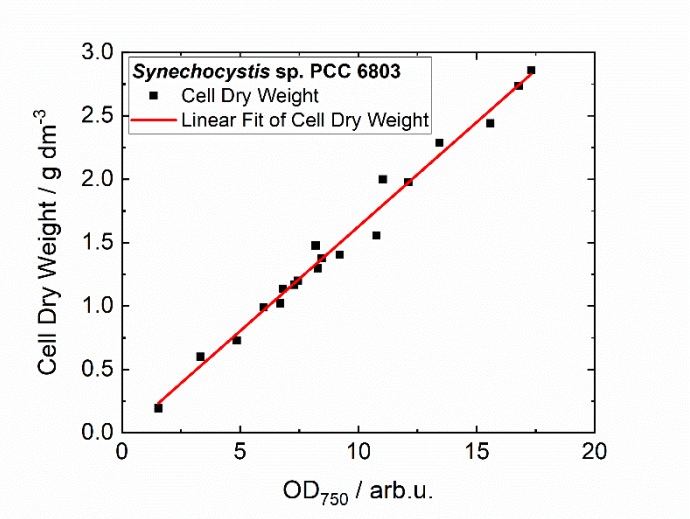

Figure S23. Determination of the correlation factor between OD_{750} and cell dry mass for Synechocystis sp. PCC 6803 via linear fitting (interception y=0). The resulting factor is 0.163 ± 0.003.

4. Experimental Setup

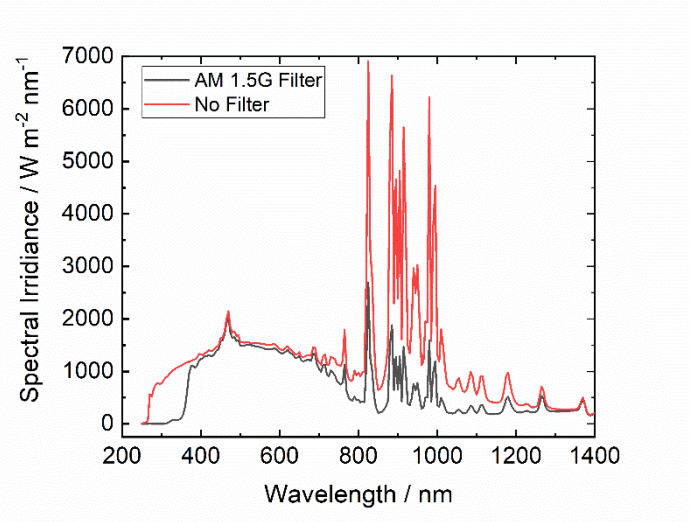

Figure S24. Spectral irridiance of the 450 W Xe-arc lamp of the sunlight simulator with (black) and without (red) AM 1.5G filter.

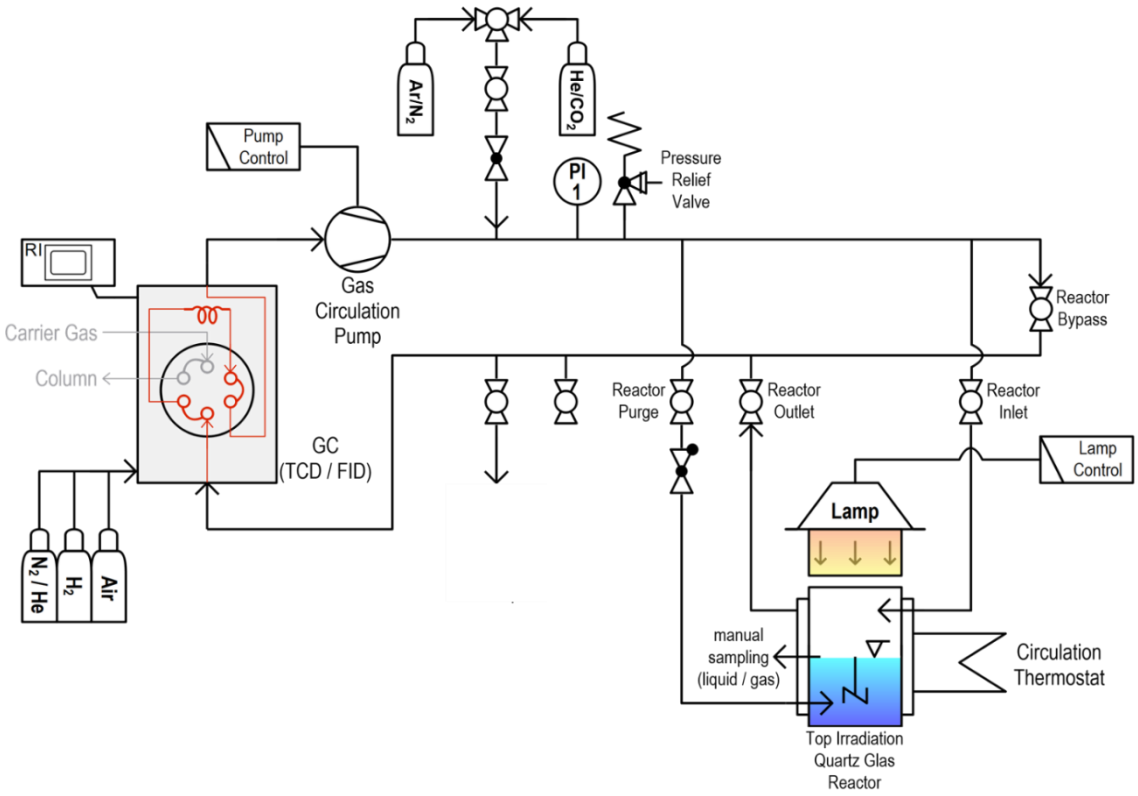

Figure S25. Flow scheme of the photocatalytic set-up, using a 450 W Xe-lamp and a Shimadzu 2010 GC with a ShinCarbon ST micropacked column. The process gas can be selected from Ar, N_2, He and CO_2.

(**a**)

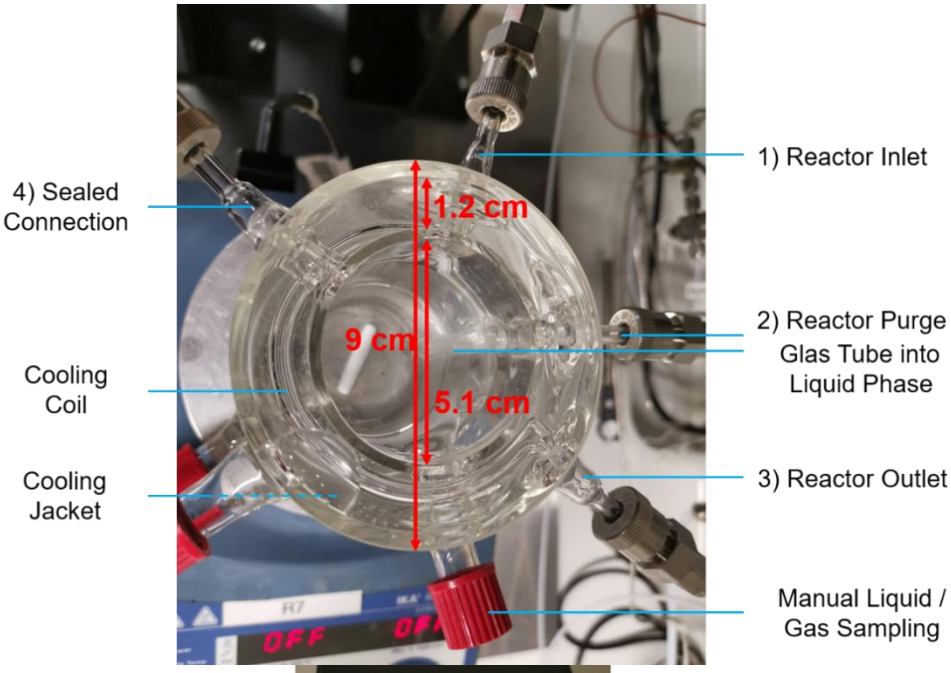

(**b**)

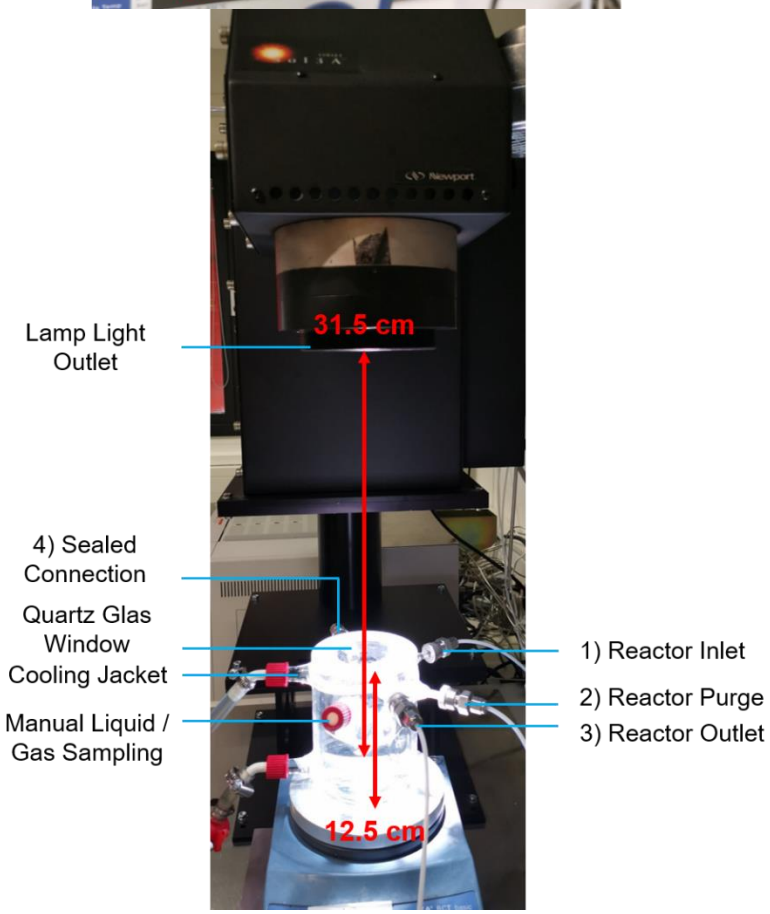

Figure S26. (**a**) Top view and (**b**) side view image of the top irradiation quartz glas cell equipped with a cooling mantle, a liquid / gas manual sample opening sealed with a PTFE septum, four gas phase inlets: 1) reactor inlet (during reaction), 2) reactor purge (before reaction), 3) reactor outlet, 4) sealed gas connection. The reactor dimensions are h = 12.5 cm (with quartz glas window), d_{total} = 9 cm, d_{in} = 5.1 cm, d_{out} = 1.2 cm. For a better visualization the reactor is filled with 100 cm^3 H_2O and

irradiated with the Xe-lamp (reactor housing for light shielding not shown). The distance between liquid phase surface and lamp opening is 31.5 cm according to manufacturer recommendations.

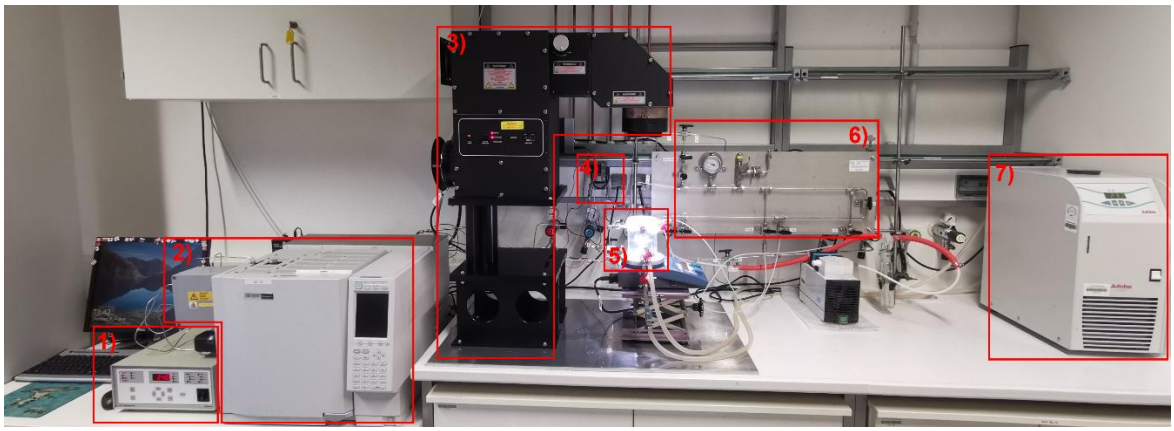

Figure S27. Image of the photocatalytic set-up. 1) Lamp power supply and control unit; 2) Shimadzu 2010 GC with a ShinCarbon ST micropacked Column and a heated sample loop; 3) sunlight simulator (450 W Xe-lamp which can be equipped with a AM 1.5G filter); 4) gas circulation pump; 5) top irradiation quartz glas reactor; 6) gas dosing system; 7) circulation thermostat.

References

1. Dang, W.; Tang, X.; Wang, W.; Yang, Y.; Li, X.; Huang, L.; Zhang, Y. Micro-nano NiO-MnCo2O4 heterostructure with optimal interfacial electronic environment for high performance and enhanced lithium storage kinetics. *Dalton Trans.* **2020**, *49*, 10994–11004, doi:10.1039/d0dt02278k.

2. Arulnesan, S.W.; Kayser, P.; Kennedy, B.J.; Knight, K.S. The impact of room temperature polymorphism in K doped NaTaO3 on structural phase transition behaviour. *J. Solid State Chem.* **2016**, *238*, 109–112, doi:10.1016/j.jssc.2016.03.008.